

FULL PAPER

Synthesis and characterization of new 4,6-dimethoxy-1*H*-indole derivatives as antibacterial and antitumor agents

Hayfaa A. Mubarak^a | Alaa Ali Hussein^b | Wisam Abdul Jaleel Jawad^c | Mustafa M. Karhib^d | Nour Abd Alrazzak^e  | Mohanad Mousa Kareem^e  | Ahmed Samir Naje^f

^aChemical Engineering Department, College of Engineering, University of Babylon, Iraq

^bCollege of Education for Girls, Department of Chemistry, University of Mosul, Iraq

^cDepartment of Chemistry, College of Science, University of Babylon, P.O. BOX 51002, Hilla, Iraq

^dDepartment of Medical Laboratory Techniques, Al-Mustaqbal University College, 51001 Hillah, Babylon, Iraq

^eDepartment of Chemistry, College of Science for Women, University of Babylon, Hilla, Iraq

^fCollege of Engineering, AlQasim Green University, Babylon, Iraq

New heterocyclic compounds derived from 4,6-Dimethoxy-1*H*-indole were synthesized. 4,6-Dimethoxy-1*H*-indole was reacted with chloroacetic acid to produce compound (R1) which used as starting material to synthesized pyrazole, isoxazole, and pyrimidine derivatives respectively. Compound (R1) reacted with urea and thiourea to produce diazetidin-2-one (R2) and diazetidine-2-thione (R3). On the other hand, (R1) was combined with thiosemecabazide to produce thiadiazole (R4) which combined with benzaldehyde in acetic acid to yield Schiff base compound (R5). This compound used as starting material to creation compounds (R6-R11) via reaction with hydrazine hydrate, phenyl hydrazine, hydroxylamine hydrochloride, acetamide, urea, and thiourea respectively. Anticancer and antibacterial activity of the synthesized compounds was investigated with good results. Compounds R3, R6, R9 and R11 with (NH) group demonstrated strong activity against MCF7 cells, the IC₅₀ values range between 31.06 - 51.23 µg/mL.

***Corresponding Author:**

Hayfaa A. Mubarak

Email: haifaadnan_81@uobabylon.edu.iq

Tel.: +9647738070652

KEYWORDS

Anticancer activity; diazetidine; isoxazole; triazolidine; pyrazoline.

Introduction

Bacteria as well as other microbial pathogens bring on the majority of infectious diseases that are fatal. Bacterial pathogens have devised a number of strategies to counteract the bactericidal and inhibitory effects of antimicrobial drugs. It is essential to maintain potent antibiotics on hand as long as in order to preserve both human and animal health. Drugs used to treat cancer and bacteria have, to some extent, lost their effectiveness due to the emergence of resistance [1,2].

Several approaches have been used recently to combat antibiotic resistance. One

of the suggested methods to accomplish this is to combine other molecules with ineffective drugs; it appears to restore the right anticancer and antibacterial activity. Because of their broad variety of biological and pharmacological properties, such as their ability to combat infection, cancer, hypertension, and inflammation of [1-3], six-membered heterocyclic rings are essential for both pharmacological and biological processes. Since they are integrated into proteins at tryptophan residues, are the building blocks of drugs like indomethacin, and act as a biologically appropriate drug store for indole alkaloids, which make up a

significant portion of natural products, indoles are vital heterocyclic molecules in medicinal chemistry [4-6]. The indole compounds have a wide range of biological activities, including antimicrobial [7], antiviral, antibacterial, and anticancer agents [8], antiarrhythmic drugs (physostigmine), and antitumor agents (vincristine) [9-11].

Many researches have been conducted on transition metal-catalyzed C-H functionalization of indoles at the C3 position in latest years, and significant advancements have been accomplished in this area [12]. The use of indoles in the direct synthesis of 3,3-diaryl benzofuranones [13], N-aryl-1-amino indoles [14], and 3,3'-diindolylmethanes (DIMs) [15] is among the most recent applications of indoles in organic synthesis.

Pyrazoles N-heterocyclic compounds (NHCps) have biological and photophysical features found in a diverse range of bioactive chemicals with the ability to be used as chemotherapeutics [16-18]. They have a hetero five-membered ring with two nitrogen atoms in the construction. Anticancer, antibacterial, antifungal, antioxidant, and anti-inflammatory properties have indeed been demonstrated for several pyrazoles [19,20].

Numerous intriguing nucleoside and nonnucleoside compounds, as well as a large variety of natural materials contain pyrimidine groups. The biological effects of pyrimidines includes antibacterial [21], antipoptotic proteins, antiviral [22], anticancer [23,24], anti-inflammatory [25-27], and analgesic characteristics.

The purpose of this effort is to develop novel 4,6-Dimethoxy-1H-indole derivatives with biological activity against bacteria and the anticancer Mcf-7.

Materials and methods

All chemicals were supplied by Merck and BDH Companies. The following techniques have been used in this study: Testseon Shimadzu (FT- IR 8400Series Japan), ¹H and

¹³CNMR Bruker, Ultra Shield 500 MHZ Switzerland.

Synthetic methods

Synthesis of 2-(4,6-dimethoxy-1H-indol-1-yl)acetic acid (R1) [28]

Chloroacetic acid (0.01 mol., 0.94 g) was dissolved in 30 mL chloroform and 4 mL pyridine in a 50 mL beaker, then (0.01 mol., 1.77 g) of compound (R) was added and refluxed for 30 hrs., then it was cooled down. The reaction was monitored by TLC and the obtained precipitate was purified by recrystallization using absolute ethanol (Table 1).

Synthesis of compounds (R2, R3) [29]

Urea (0.01 mol., 0.60 g), thiourea (0.01 mol., 0.76 g) and (0.01 mol., 1.06 g) Na₂CO₃ were mixed in absolute ethanol (20 mL) and added to compound (R1) (0.01 mol., 2.35 g). the mixture was refluxed for 5 hours, then added in ice water and stirred for 30 minutes. The reaction was monitored by TLC and the precipitate was purified by recrystallization using absolute ethanol (Table 1).

Synthesis of compound (R4) [30]

Thiosimicarbazide (0.01 mol., 0.91 g) was combined with 50 mL (10%) NaOH solution and the mixture was stirred for 20 minutes. A solution of 50 mL of dioxin and (0.01 mol., 2.35 g) of (R1) was added to the mixture and refluxed for 24 hours. Ice water and concentrated HCl were added and stirred for 30 minutes. TLC used for monitoring the reaction and the formed precipitate was purified by recrystallization using absolute ethanol (Table 1).

Synthesis of compound (R5) [30]

Benzaldehyde (0.01 mol., 1.06 g) was added to a mixture of compound (R4) (0.01 mol., 2.90 g), glacial acetic acid (2 drops) and ethanol (20

mL) and refluxed for 4 hours. TLC used for monitoring the reaction and the formed precipitate was purified by recrystallization using absolute ethanol (Table 1).

Synthesis of compounds (R6, R7) [30]

Compound (R5) (0.005 mol.), and hydrazine hydrate (0.005 mol., 0.25 mL) of, phenylhydrazine were dissolved in (50 mL) ethanol. The mixture was refluxed for a period of time (12 hrs.). TLC used for monitoring the reaction and the formed precipitate was purified by recrystallization using absolute ethanol (Table 1).

Synthesis of compound (R8) [30]

Ethanol (50 mL), (0.02 mol.) compound (R5), (0.02 mol., 1.4 g) hydroxylamine

hydrochloride, KOH (2.0 g), and water (5 mL) were mixed. The mixture was refluxed for (24 hrs.). Then, the mixture was cooled, filtered, and recrystallized using ethanol-water solvent (Table 1).

Synthesis of compounds (R9, R10, R11) [31]

Small piece of sodium metal was dissolved in (25 mL) of absolute ethanol, and then (0.01 mol.) of acetamide, urea or thiourea was added. In another flask, compound (R5) (0.02 mol.) was dissolved in (25 mL) absolute ethanol. Both solutions were mixed and refluxed for 24 hours. The reaction was cooled and the solid product was filtered off and recrystallized from ethanol (Table 1). Synthesis of the compounds (R1-R11) presented in Scheme 1.

TABLE 1 Physical properties of the compounds (R1-R11).

Comp. No.	Molecular Formula	M.Wt	Color	m.p. °C	Yield%	R _f	(TLC)
R1	C ₁₂ H ₁₃ NO ₄	235.24	Pale yellow	107-109	86	0.47	n-hexane: DCM 1:1
R2	C ₁₄ H ₁₇ N ₃ O ₃	275.30	Dark orange	178-179	83	0.77	Acetone:n-hexane 1:1
R3	C ₁₃ H ₁₅ N ₃ O ₂ S	277.34	Yellow-Orange	126-128	68	0.85	n-hexane:acetone 1:1
R4	C ₁₃ H ₁₅ N ₄ O ₂ S	291.35	Dark orange	132-134	75	0.68	n-hexane:acetone 1:2
R5	C ₂₀ H ₁₈ N ₄ O ₂ S	378.45	White	98-100	76	0.58	Benzene:Ethyl acetate 3:1
R6	C ₂₁ H ₂₀ N ₄ O ₂ S	392.47	Off-white	168-169	66	0.71	Petroleum ether :CHCl ₃ 3:3
R7	C ₂₇ H ₂₄ N ₄ O ₂ S	468.57	White	180-182	88	0.79	n-hexane:DCM 1: 1
R8	C ₂₁ H ₁₉ N ₃ O ₃ S	393.46	Bright Brown	151-153	79	0.77	n-hexane:DCM 1: 1
R9	C ₂₃ H ₂₁ N ₃ O ₃ S	419.49	Green-Yellow	127-129	68	0.57	Acetone: hexane 1:1
R10	C ₂₂ H ₂₀ N ₄ O ₃ S	420.48	Light brown	116-118	75	0.85	Hexane:acetone 3:3
R11	C ₂₂ H ₂₀ N ₄ O ₃ S ₂	452.54	Yellowish Brown	174-176	80		Hexane:acetone 3:3

Results and discussion

We developed a new series of 4, 6-dimethoxy-1H-indole chemical derivatives in this study that have functional groups (pyrazole, isoxazole, and pyrimidine) (scheme1). FTIR, ¹H&¹³C-NMR, and CHNS techniques were used to validate the structures of the novel compounds (R1-R11). We looked into how

they responded to microorganisms and the anticancer MCF-7. Compound R1: FTIR spectrum shows disappearance of NH group at (3216 cm⁻¹), (OH) of acid at 3366-2400 cm⁻¹, (CH_{ar}) at 3080 cm⁻¹, (CH_{alph}) at 2908 cm⁻¹, 1581 cm⁻¹ (C=C)_{ar}, (C-N) at 1382 cm⁻¹, (C-O) at 1254-1207 cm⁻¹. ¹H-NMR spectrum, revealed an appearance singlet (COOH) at 11.90 ppm, 3.93, 3.94 ppm for (CH₃-O) group, CH₂-N group

at (4.57) ppm, (CH)_{ar}. at (6.48 -7.76) ppm (Figure 1). The Elemental Analysis C₁₂H₁₃NO₄

(Calc.), founded: C% (61.27) 60.10; H% (5.57) 5.18; N% (5.95) 5.37.

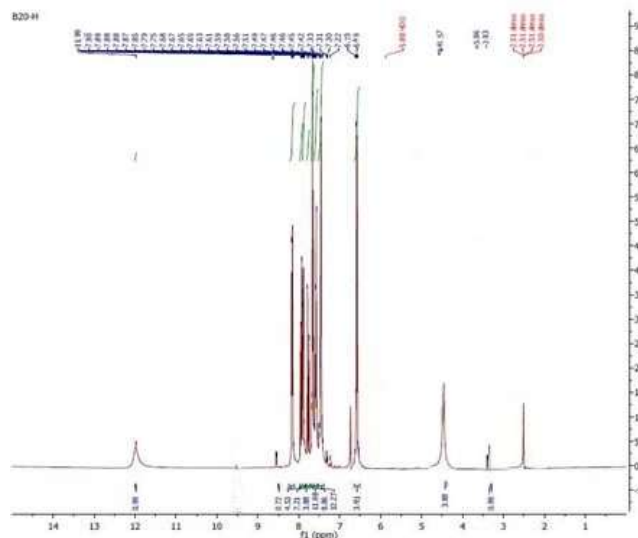


FIGURE 1 ¹H-NMR spectrum of compound (R1)

Compound (R2): FTIR spectrum shows appearance NH band at 3243 cm⁻¹, (C-H)_{ar} at 3031 cm⁻¹, (CH)_{alph} at 2951, 2847 cm⁻¹, 1515, 1601 cm⁻¹ (C=C)_{ar}, (NH-C=O) 1614, (C-N) 1401 cm⁻¹, and (C-O) 1130-1284 cm⁻¹. ¹H-NMR spectrum shows appearance singlet peak

(CH₃-O) at 3.59 ppm, 3.66 ppm, (CH)_{ar}. at 6.20 -7.96 ppm, (-NH) at 6.72 ppm, (-CH₂) at 4.33 ppm, (CH₂-N) at 5.98 ppm (Figure 2). The Elemental Analysis C₁₄H₁₇N₃O₃ (Calc.), founded: C% (61.08) 60.20; H% (6.22) 5.97; N% (15.26) 14.75.

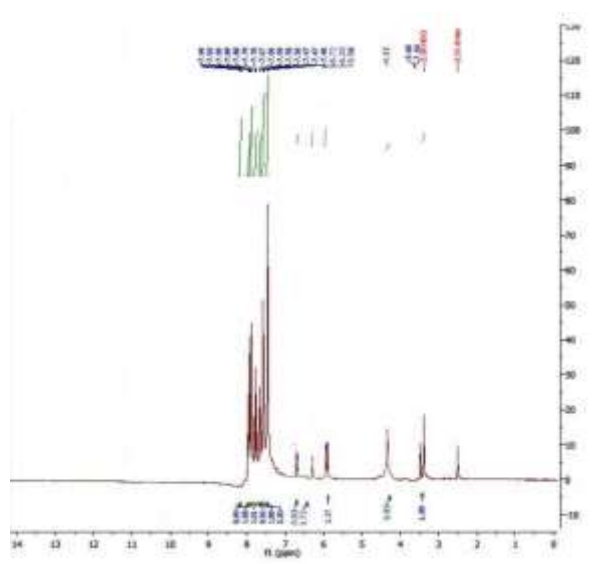


FIGURE 2 ¹H-NMR spectrum of compound (R2).

Compound (R3): FTIR spectrum shows -NH band at 3155 cm⁻¹, (C-H)_{ar} at 3028 cm⁻¹, (CH)_{alph} at 2981 cm⁻¹, (C=C)_{ar}. 1537 cm⁻¹, (C=S) 1595, (C-N) 1369 cm⁻¹, and (C-O) 1103 cm⁻¹-1016 cm⁻¹. ¹H-NMR spectrum:

appearance singlet : (CH₃-O) 3.47, 3.48 ppm and (CH) _{ar}. 6.42-7.88 ppm, (-NH) 6.72 ppm, (CH) 2.63 ppm, (CH₂-N) 5.21 ppm (Figure 3). The Elemental Analysis C₁₃H₁₅N₃O₂S (Calc.),

founded: C% (56.3) 54.9; H% (5.45) 5.15; N% (15.15) 14.50; S% (11.56) 10.88.

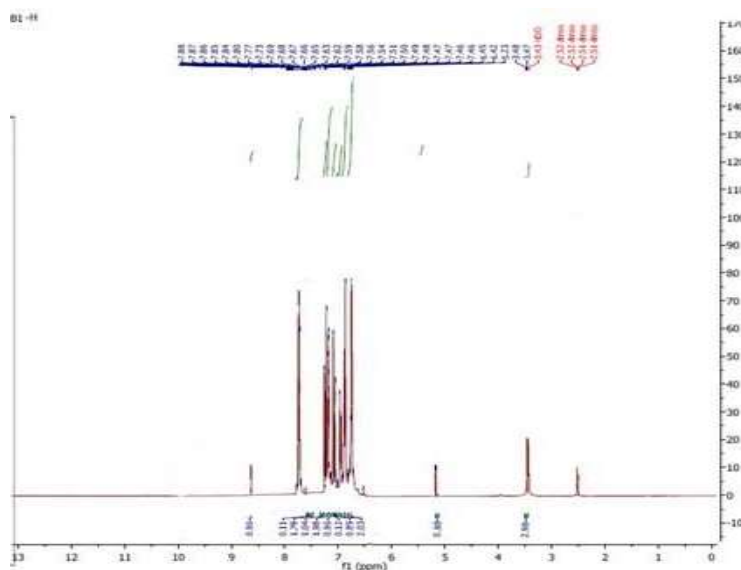


FIGURE 3 ^1H NMR spectrum of compound (R3)

Compounds R4 and R5: FTIR spectrum shows appearance of NH_2 band at $3404\text{--}3363\text{ cm}^{-1}$, $(\text{CH})_{\text{ar}}$ 3037 cm^{-1} , $(\text{C}=\text{N})$ 1604 cm^{-1} , $(\text{C}=\text{C})_{\text{ar}}$ $1545\text{--}1515\text{ cm}^{-1}$, $(\text{C}-\text{N})$ ($1278\text{--}1107$) cm^{-1} , $(\text{C}-\text{S})$ 1484 cm^{-1} . ^1H NMR spectrum: disappearance singlet COOH at 11.90 ppm in (R1), appearance signal NH_2 at 6.53 ppm , $(\text{N}-\text{CH}_2)$ at 5.43 ppm , and (CH_3-O) at 3.61 ppm , 3.63 ppm , and $(\text{CH})_{\text{ar}}$ at $(6.43\text{--}7.81)\text{ ppm}$. ^{13}C NMR spectrum: $(\text{CH}_2-\text{N}, \text{CH}_3-\text{O})$ signal at $65.11, 65.00\text{ ppm}$, (CH_{ar}) at $122.56\text{--}135.14\text{ ppm}$, $(\text{C}=\text{N})$ at $165.87, 157.38, 154.38\text{ ppm}$ (figure 4). The Elemental Analysis $\text{C}_{13}\text{H}_{15}\text{N}_4\text{O}_2\text{S}$ (Calc.), founded: C% (53.59) 52.80; H% (5.19) 4.85; N% (19.23) 18.70; S% (11.00) 10.55.

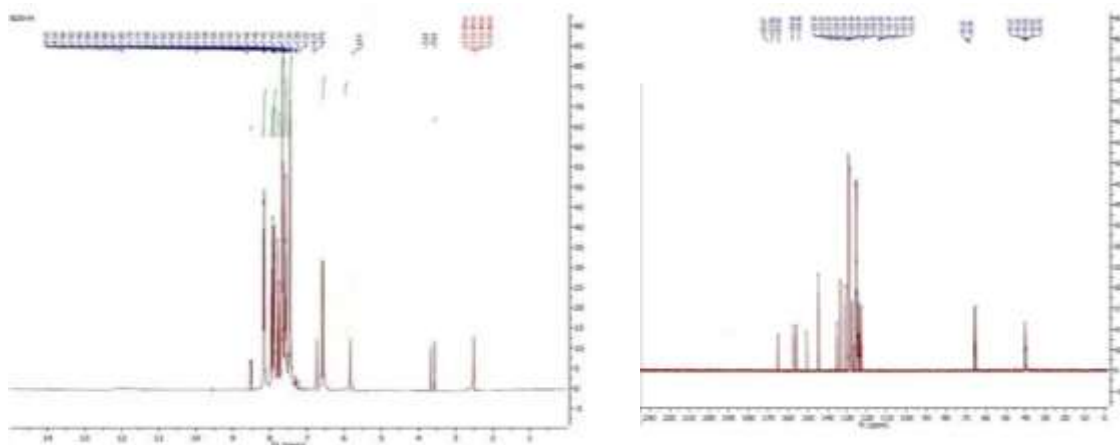
FTIR spectrum of R5 shows (NH_2) group appeared at 3433 cm^{-1} of R4, $(\text{CH}_{\text{alph}})$ at $2939\text{--}2981\text{ cm}^{-1}$, (CH_{ar}) at 3059 cm^{-1} , $\text{C}=\text{N}$ at 1670 cm^{-1} , $(\text{C}-\text{N})$ 1377 cm^{-1} , $(\text{C}-\text{O})$ $1203\text{ cm}^{-1}\text{--}1246\text{ cm}^{-1}$, and $\text{C}=\text{Car}$. $1558\text{--}1489\text{ cm}^{-1}$. ^1H NMR spectrum of compound R5 displayed a signal of appearance CH_3-O at $3.85\text{ ppm}, 3.84\text{ ppm}$, $(\text{CH})_{\text{ar}}$ at $6.04\text{--}7.96\text{ ppm}$, $(\text{CH}=\text{N})$ at 8.22 ppm , and (CH_2-N) 4.83 ppm . ^{13}C NMR spectrum of compound R5 displayed a signal of appearance (CH_3-O) $61.06\text{ ppm}, 62.26\text{ ppm}$, (CH_2-N) 66.12 ppm , (Car) $112.09\text{--}129.37\text{ ppm}$,

$(\text{CH}-\text{N})$ 164.99 ppm , $(\text{C}=\text{N})$ $164.45, 154.50\text{ ppm}$ (Figure 4). The Elemental Analysis $\text{C}_{20}\text{H}_{18}\text{N}_4\text{O}_2\text{S}$ (Calc.), founded: C% (63.47) 63.05; H% (4.79) 4.25; N% (14.8) 14.40; S% (8.47) 8.07.

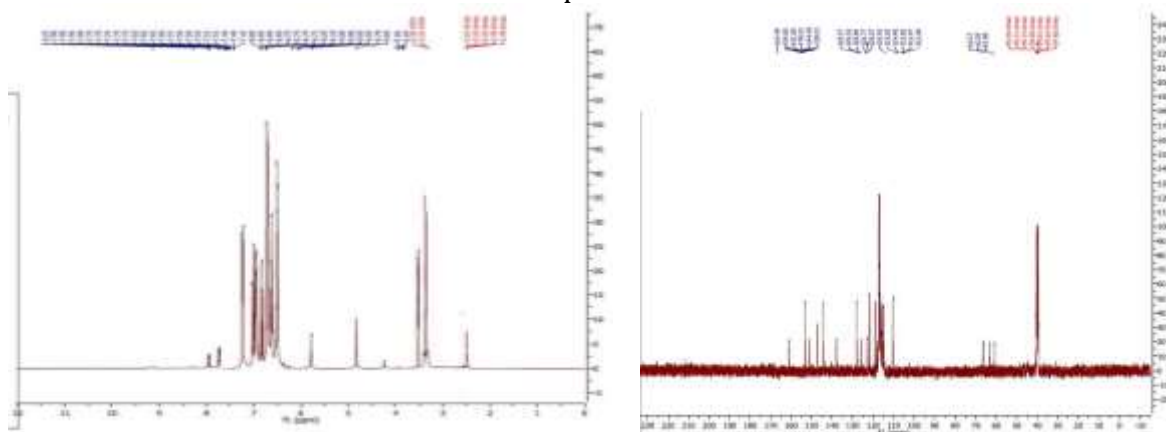
Compounds (R6 and R7): FTIR spectra of compounds (R6 and R7) shows appearance bands of NH group at 3241 cm^{-1} , $(\text{C}=\text{N})$ group at $1634\text{ cm}^{-1}, 1650\text{ cm}^{-1}$, $(\text{C}=\text{C})$ $1573\text{ cm}^{-1}, 1604\text{--}1492\text{ cm}^{-1}$, $(\text{CH}_{\text{alph}})$ 2947 cm^{-1} , (Char.) $3051\text{ cm}^{-1}, 1446\text{ cm}^{-1}$, $(\text{C}-\text{N})$ 1373 cm^{-1} , and $(\text{C}-\text{O})$ 1211 cm^{-1} . ^1H -NMR spectrum showed CH_3-O signal at $3.30\text{ ppm}, 3.40\text{ ppm}$, $(\text{CH})_{\text{ar}}$ at $6.26\text{--}7.88\text{ ppm}$, (NH) at 7.63 ppm , (CH_2-N) 4.86 ppm , and $(\text{CH}-\text{N})$ 2.45 ppm (Figure 5). The Elemental Analysis $\text{C}_{21}\text{H}_{20}\text{N}_4\text{O}_2\text{S}$ (Calc.), founded: C% (64.27) 63.75; H% (5.14) 5.05; N% (14.28) 13.90; and S% (8.17) 7.77.

^1H -NMR spectrum of compounds, R7 shows CH_3-O signal at 3.45 ppm , $(\text{CH})_{\text{ar}}$ at $6.54\text{--}7.98\text{ ppm}$, $(\text{CH}-\text{N})$ at 3.90 ppm , (CH_2-N) 3.91 ppm , and $(\text{CH}-\text{N})$ 1.98 ppm . ^{13}C NMR spectrum of (R7) displayed a signal of appearance (CH_2-N) at 526.00 ppm , (Car.) $112.09\text{--}135.03\text{ ppm}$, $(\text{C}-\text{N})$ 65.94 ppm , $(\text{N}=\text{C})$ $158.01\text{ ppm}, 154.40\text{ ppm}$, and $(\text{N}=\text{C}-\text{S})$ at 164.34 ppm (figure). The Elemental Analysis $\text{C}_{27}\text{H}_{24}\text{N}_4\text{O}_2\text{S}$ (Calc.),

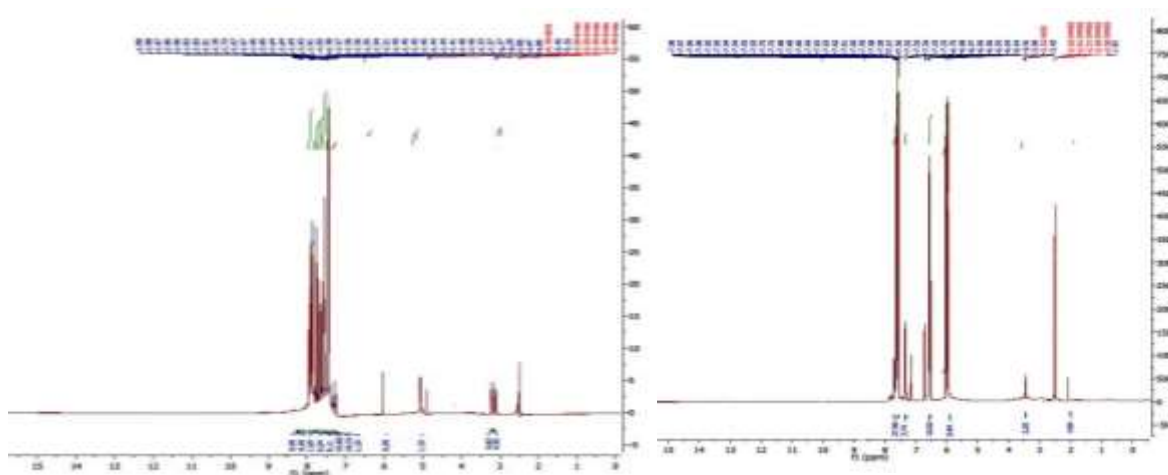
founded: C% (69.21) 68.85; H% (5.16) 5.01;
N% (11.96) 11.50; and S% (6.84) 6.57).



Compound R4



Compound R5

FIGURE 4 ^1H NMR and ^{13}C NMR spectra of compounds R4 and R5

Compound R6

Compound R7

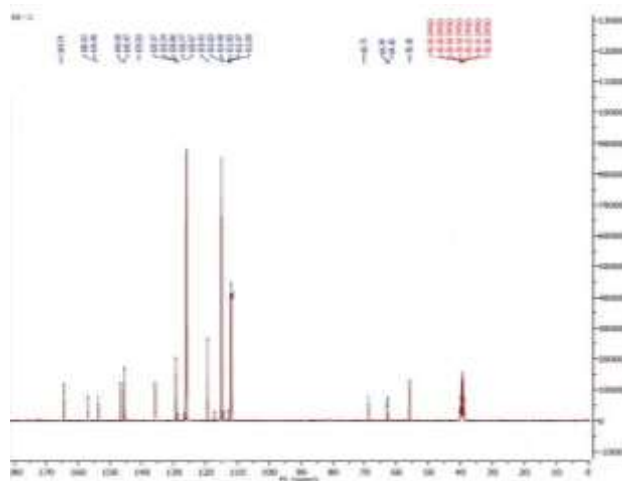
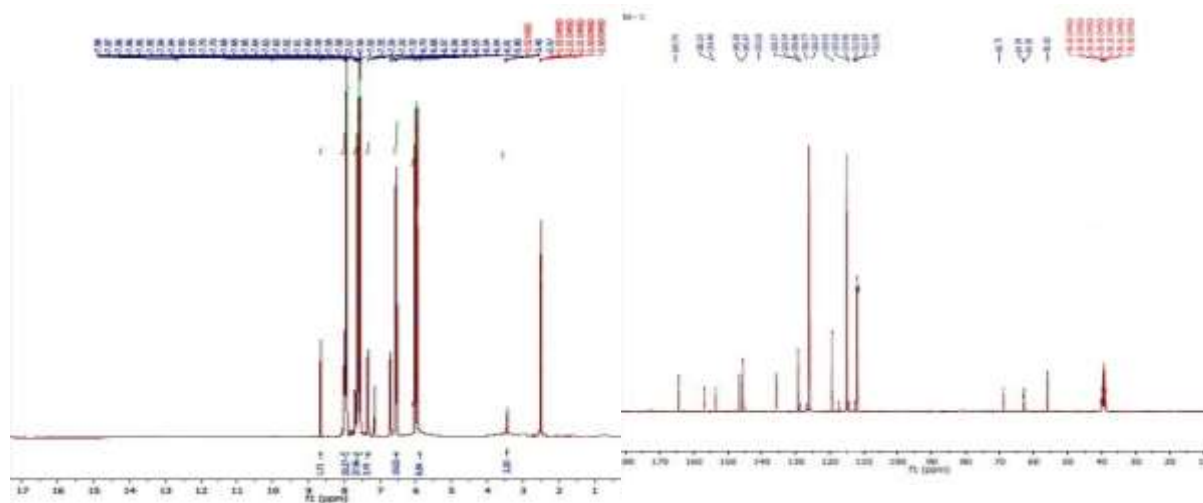


FIGURE 5 ^1H NMR of compounds R6, R7 and ^{13}C NMR of compound R7 spectra.

Compounds R8 and R9: FTIR spectrum of (R8) appearance of new absorption stretching bands of NH group at 3241 cm^{-1} , (C=N) group 1634 cm^{-1} , 1650 , (C=C) ar. 1573 cm^{-1} , 1604 - 1492 cm^{-1} , (CH_{alph}) at 2947 cm^{-1} , 2980 cm^{-1} , (CHar) at 3051 cm^{-1} , 1446 cm^{-1} , 1373 cm^{-1} (C-N), 1211 cm^{-1} (C-O). ^1H NMR spectrum of compound R8: signal $\text{CH}_3\text{-O}$ at 3.45, 3.44 ppm, (CH)ar. at 6.01-7.98 ppm, ($\text{CH}_2\text{-N}$) 5.90 ppm,

and (CH-N) at 2.67 ppm. ^{13}C NMR spectrum (R8) appearance signal ($\text{CH}_2\text{-N}$) at 57.68 ppm, (Car.) at 122.28-135.49 ppm, (C-N) at 65.11 ppm, (N=C) 157.38 ppm, 154.38 ppm, (N=C-S) at 165.89 ppm (Figure 6). The Elemental Analysis $\text{C}_{21}\text{H}_{19}\text{N}_3\text{O}_3\text{S}$ (Calc.), founded: C% (64.11) 63.82; H% (4.87) 4.71; N% (10.68) 10.52; S% (8.15) 8.07.



compound R8

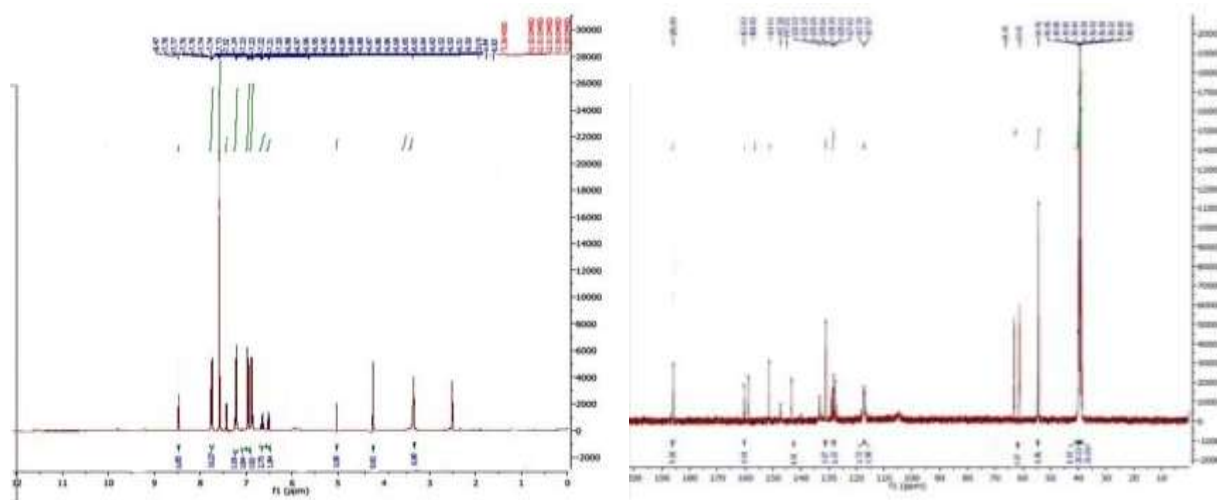
FIGURE 6 ^1H NMR and ^{13}C NMR spectra of compound R8

FTIR spectrum of compound R9 display absorption band for (C=O) at 1702 , 1633 cm^{-1} , (C=C) 1570 cm^{-1} , (N-H) at 3116 cm^{-1} , (C=C) ar. 1570 cm^{-1} , (CH_{alph}) at 2916 cm^{-1} , 2809 cm^{-1} , (CHar) at 3051 cm^{-1} , (C-N) 1368 cm^{-1} , (C-O) 1290 - 1129 cm^{-1} . ^1H NMR spectrum of R9

display signal: $\text{CH}_3\text{-O}$ at 3.99 ppm, (CH)ar. at 6.50-7.79 ppm, (NH) at 8.15 ppm, ($\text{CH}_2\text{-N}$) 4.49 ppm, (=CH) 5.18 ppm, and (CH-N) 2.65 ppm. ^{13}C NMR spectrum of R9: ($\text{CH}_2\text{-N}$) signal at 54.41 ppm, (Car.) 117.28-133.19 ppm, (C-N) 61.41 ppm, (N=C) 153.11 ppm, (N=C-S) 162.63

ppm (Figure 7). The Elemental Analysis $C_{23}H_{21}N_3O_3S$ (Calc.), founded: C% (65.85)

64.12; H% (5.05) 4.91; N% (10.02) 9.62; S% (7.64) 7.17.

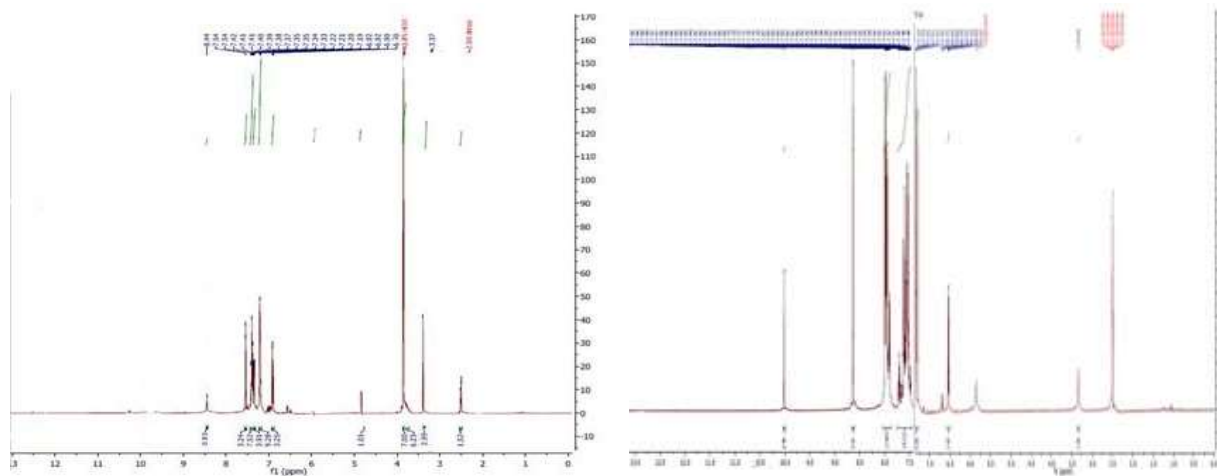


compound R9

FIGURE 7 1H NMR and ^{13}C NMR spectra of compound R8 and R9.

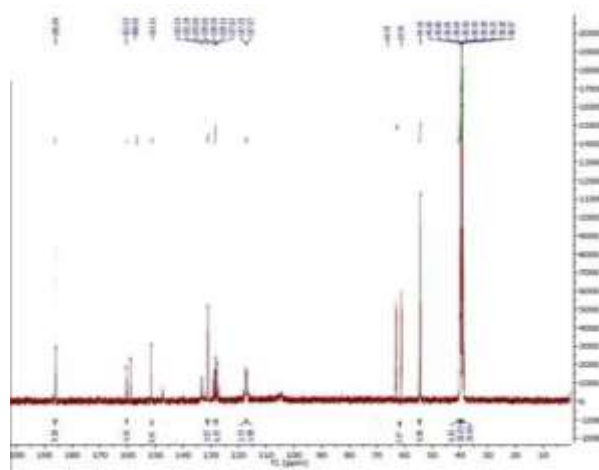
Compounds (R10, R11): FTIR spectra of compounds (R10, R11), shows absorption band (NH) band at 3323 cm^{-1} , 3255 cm^{-1} , (C=S) 1136 cm^{-1} , (C=O) 1665 cm^{-1} , 3037 cm^{-1} , 2999 cm^{-1} to Char., (C=N) 1610 cm^{-1} , (C=Car) $1605, 1535\text{ cm}^{-1}$, (C-N) 1376 cm^{-1} , 1375 cm^{-1} , (C-S) 1450 cm^{-1} . 1H -NMR spectrum of R10 display a peak for CH_3-O group at 3.37 ppm, (CH)ar. 6.39-7.54 ppm, (NH) at 8.44 ppm, (CH_2-N) 4.39 ppm, and (CH-N) 2.65 ppm. The Elemental Analysis $C_{22}H_{20}N_4O_3S$ (Calc.), founded: C% (62.84) 61.22; H% (4.79) 4.44;

N% (13.32) 12.22; S% (7.62) 7.27. 1H -NMR spectrum of R11: CH_3-O signal at 3.34 ppm, (CH)ar. 6.71-8.63 ppm, (NH) at 10.00 ppm, (CH) 6.53 ppm. ^{13}C -NMR spectrum of R11: (CH_2-N) display signal at 62.63 ppm, (Car) 117.07-133.31 ppm, (CH-N) at 64.41 ppm, (CH_3-O) 56.99 ppm, 54.41 ppm, 154.31 ppm to (N=C), (N=C-S) 162.63 ppm, (S=C) 185.87 ppm (Figure 8). The Elemental Analysis $C_{22}H_{20}N_4O_3S_2$ (Calc.), founded: C% (58.39) 58.21; H% (4.45) 4.24; N% (12.38) 12.20; S% (14.17) 13.97.



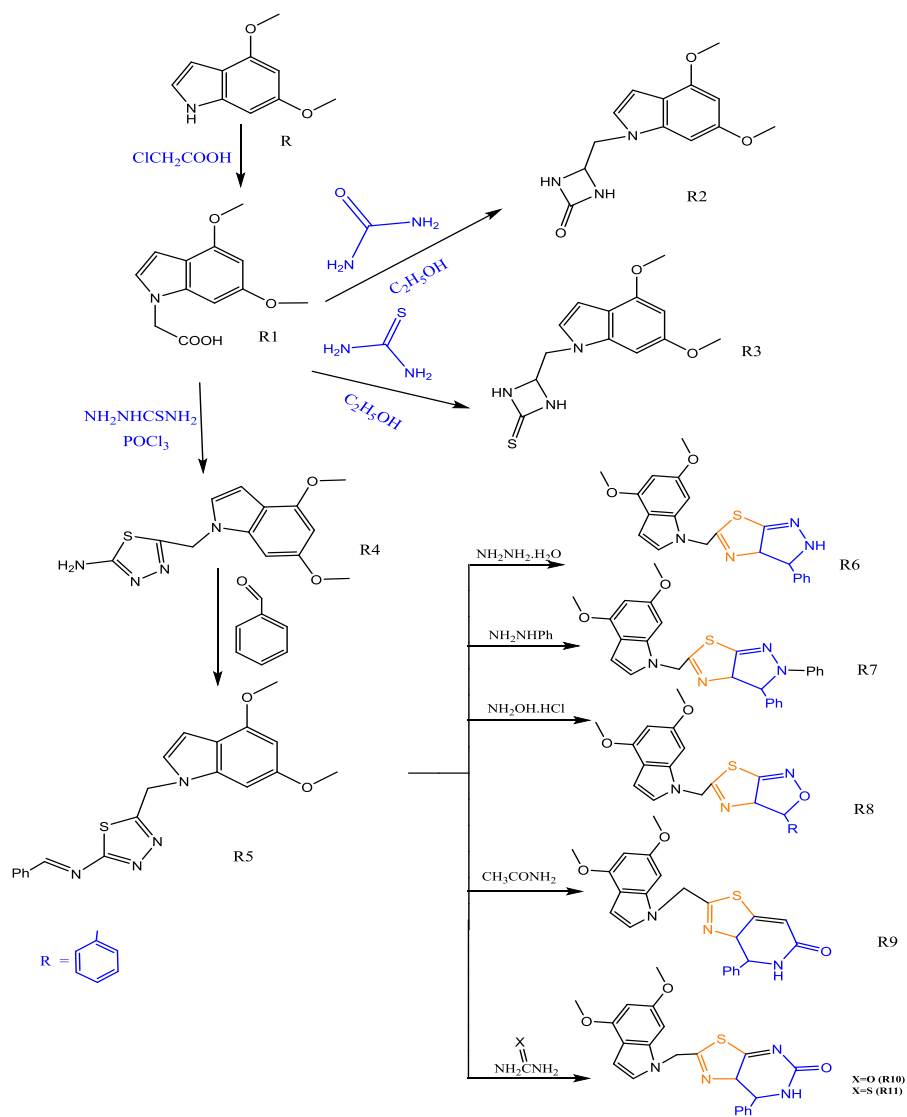
Compound R10

Compound R11



Compound R11

FIGURE 8 ¹H NMR OF R10, R11 and ¹³C NMR of compound R11 spectra



SCHEME 1 Synthesis of compounds (R1-R11)

Solubility of the synthesized compounds

The synthesized compounds were insoluble in diethyl ether, petroleum ether, acetone and hexane but showed a good solubility in DMSO and DMF. Some prepared compounds are

somewhat soluble in ethanol, water, and ethyl acetate. Solubility properties of prepared compounds in different solvents (H₂O, ethanol, CH₂Cl₂, ether, petroleum ether, DMSO, hexane, DMF, ethyl acetate and acetone) are listed in Table 2.

TABLE 2 Solubility of the synthesized compounds (R1-R11) in different solvents

Comp.	DMSO	DMF	DCM	Pet. ether	Ethyl acetate	Acetone	Di ethyl ether	H ₂ O	Hexane	EtOH
R1	+	+	-	Partial	Partial	Partial	-	Partial	Partial	+
R2	+	+	+	Partial	+	-	-	Partial	-	Partial
R3	+	+	-	Partial	Partial	Partial	-	+	-	+
R4	+	+	-	-	Partial	+	-	Partial	-	Partial
R5	+	+	+	-	Partial	Partial	-	Partial	Partial	Partial
R6	+	+	Partial	Partial	+	Partial	-	+	Partial	Partial
R7	+	+	+	-	-	Partial	-	Partial	-	+
R8	+	+	Partial	Partial	Partial	+	-	Partial	Partial	Partial
R9	+	+	+	Partial	Partial	Partial	-	+	Partial	Partial
R10	+	+	Partial	-	+	-	-	+	Partial	+
R11	+	+	+	-	-	Partial	-	Partial	-	+

Antibacterial Activity of the synthesized derivatives (R1-R10)

Using gram-positive (E-coli) and gram-negative bacteria (Staph. Aureu.), It was looked at how effective some synthetic substances were against microorganisms. The

derivatives (R1, R4, R5, R6, R7, R9, R10) have a good effectiveness in inhibiting the growth of (G-). The compounds (R1, R2, R3, R5, R6, R7, R8) have a good effectiveness in inhibiting bacteria (G+) in comparison with Cefotaxime, as listed in Table 3 [30].

TABLE 3 Antibacterial activity of compounds (R1-R10)

Comp. No.	<i>Escherichia coli</i> (inhibition zone mm)	<i>Staphylococcus aureus</i> (inhibition zone mm)
Cefotaxime (Antibiotic) Standard	11	16
R1	13	18
R2	8	20
R3	9	21
R4	15	17
R5	16	10
R6	13	24
R7	15	23
R8	8	17
R9	14	10
R10	14	14

Anticancer activity of the synthesized derivatives (R3, R6, R9, R11)

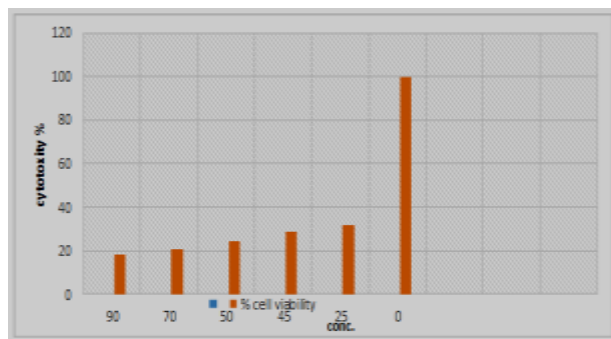
The anti-proliferating activity of the synthesized compounds (R3, R6, R9, R11)

against breast cancer cell lines (MCF-7) was studied in this investigation. The cytotoxicity analyzes of these compounds are suitable for

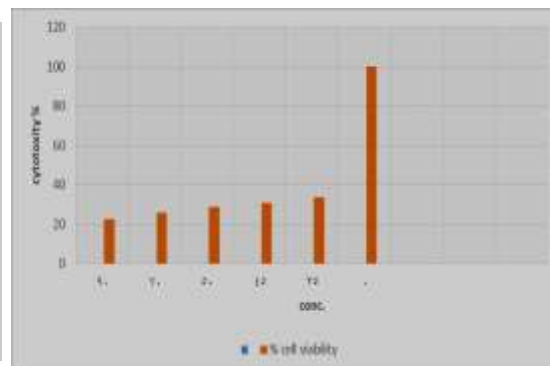
clinical application against breast cancer (Eq. 1).

In comparison with other studies, the IC50 value was much lower (R3=31.06, R6=33.66, R9=42.18, R11=51.23) and triggered

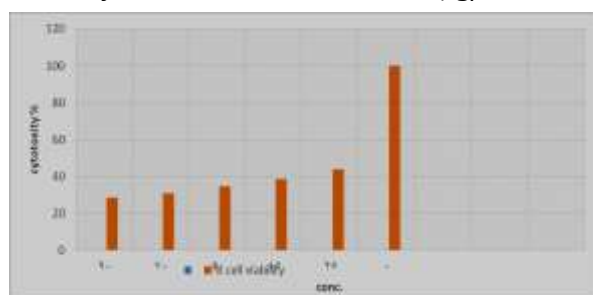
apoptotic cell death (Figure 9). The following equation was used to calculate the rate of cell growth inhibition (cytotoxicity percentage) [32].



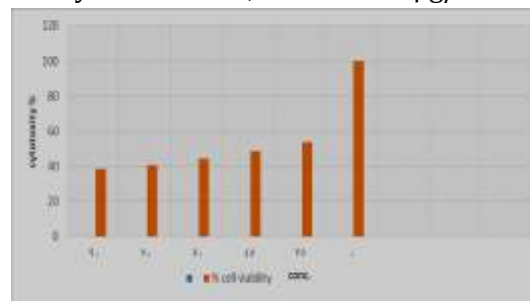
Cytotoxic of R3, IC50=31.06 $\mu\text{g}/\text{mL}$



Cytotoxic of R6, IC50=33.66 $\mu\text{g}/\text{mL}$



Cytotoxic of R9, IC50=42.18 $\mu\text{g}/\text{mL}$



Cytotoxic of R11, IC50= 51.23 $\mu\text{g}/\text{mL}$

FIGURE 9 Cytotoxic of R3, R6, R9, and R11

Conclusion

Based on 4,6-Dimethoxy-1*H*-indole, a number of novel compounds were created and then various methods were used to describe them. The outcomes showed that indole was the source of the novel pyrazole, isoxazole, and pyrimidine. These substances were examined for their antibacterial efficacy against a variety of harmful bacterial species, and the results suggest that a number of these derivatives had strong antimicrobial activity. The cytotoxic potential of derivatives against MCF7 produced conclusive evidence that the derivatives R3, R6, R9, and R11 are active substances against MCF7.

Acknowledgements

The authors thank their universities for project funding.

Conflict of Interest

The authors declare that they have no conflict of interest.

Orcid:

Mohanad Mousa Kareem:

<https://orcid.org/0000-0003-4931-5524>

Nour Abd Alrazzak:

<https://orcid.org/0000-0003-0711-3211>

References

- [1] M. Gaikwad, S. Gaikwad, R. Kamble, Synthesis of Novel Series of 1-(6-Hydroxy-4-(1*H*-indol-3-yl)-3,6-dimethyl-4,5,6,7-tetrahydro-1*H*-indazol-5-yl)ethan-1-one as Evaluations of their Antimicrobial Activity with Insilco Docking Study, *J. Med. Chem. Sci.*, **2022**, *5*, 239-248. [Crossref], [Google Scholar], [Publisher]

- [2] M. Sathiyaraj, P. Venkatesh, Ultrasound assisted synthesis of N-aryl indole under multi-site phase-transfer catalyst: A kinetic study, *J. Med. Chem. Sci.*, **2019**, *2*, 27-34. [[Crossref](#)], [[Google Scholar](#)], [[Publisher](#)]
- [3] R. Shinde, V. Adole, Anti-microbial evaluation, Experimental and Theoretical Insights into Molecular Structure, Electronic Properties, and Chemical Reactivity of (E)-2-((1H-indol-3-yl)methylene)-2,3-dihydro-1H-inden-1-one, *Appl. Organomet. Chem.*, **2021**, *1*, 48-58. [[Crossref](#)], [[Google Scholar](#)], [[Publisher](#)]
- [4] S.M. Umer, M. Solangi, K.M. Khan, R.S.Z. Saleem, Indole-containing natural products 2019–2022: isolations, reappraisals, syntheses, and biological activities, *Molecules*, **2022**, *27*, 7586. [[Crossref](#)], [[Google Scholar](#)], [[Publisher](#)]
- [5] A. Zarkan, J. Liu, M. Matuszewska, H. Gaimster, D.K. Summers, Local and universal action: The paradoxes of indole signalling in bacteria, *Trends Microbiol.*, **2020**, *28*, 566–577. [[Crossref](#)], [[Google Scholar](#)], [[Publisher](#)]
- [6] T. Wang, X. Zheng, H. Ji, T.L. Wang, X.H. Xing, C. Zhang, Dynamics of transcription–translation coordination tune bacterial indole signaling, *Nat. Chem. Biol.* **2020**, *16*, 440-449. [[Crossref](#)], [[Google Scholar](#)], [[Publisher](#)]
- [7] A. Kumar, V. Sperandio, Indole signaling at the host-microbiota-pathogen interface, *MBio*, **2019**, *10*, 01031-19. [[Crossref](#)], [[Google Scholar](#)], [[Publisher](#)]
- [8] A.G. Atanasov, S.B. Zotchev, V.M. Dirsch, International natural product sciences taskforce, *Nat. Rev. Drug Discov.*, **2021**, *20*, 200–216. [[Google Scholar](#)], [[Publisher](#)]
- [9] C. Kiesecker, E. Zitron, S. Luck, R. Bloehs, E.P. Scholz, S. Kathofer, D. Thomas, V.A. Kreye, H.A. Katus, W. Schoels, C.A. Karle, J. Kiehn, Class Ia anti-arrhythmic drug ajmaline blocks HERG potassium channels: mode of action, *Naunyn Schmiedebergs Arch. Pharmacol.* **2004**, *370*, 423–435. [[Crossref](#)], [[Google Scholar](#)], [[Publisher](#)]
- [10] P.W. Moore, J.J. Rasimas, J.W. Donovan, Physostigmine is the antidote for anticholinergic syndrome, *J. Med. Toxicol.*, **2015**, *11*, 159–160. [[Crossref](#)], [[Google Scholar](#)], [[Publisher](#)]
- [11] A.A. Ibrahim, M.M. Kareem, T.H. Al-Noor, T. Al-Muhimeed, A.A. AlObaid, S. Albukhaty, G.M. Sulaiman, M. Jabir, Z.J. Taqi, U.I. Sahib, Pt(II)-Thiocarbohydrazone Complex as Cytotoxic Agent and Apoptosis Inducer in Caov-3 and HT-29 Cells through the P53 and Caspase-8 Pathways, *Pharmaceuticals*, **2021**, *14*, 509. [[Crossref](#)], [[Google Scholar](#)], [[Publisher](#)]
- [12] P. Kumar, P.J. Nagtilak, M. Kapur, Transition metal-catalyzed C–H functionalizations of indoles, *New J. Chem.*, **2021**, *45*, 13692–13746. [[Crossref](#)], [[Google Scholar](#)], [[Publisher](#)]
- [13] Z. Tang, Z. Liu, Z. Tong, Z. Xu, C.T. Au, R. Qiu, N. Kambe, Cu-catalyzed cross-dehydrogenative coupling of heteroaryl construction of all-carbon triaryl quaternary centers, *Org. Lett.*, **2019**, *21*, 5152–5156. [[Crossref](#)], [[Google Scholar](#)], [[Publisher](#)]
- [14] Y. Ou, T. Yang, N. Tang, S.-F. Yin, N. Kambe, R. Qiu, Photo-induced N–N coupling of *o*-nitrobenzyl alcohols and indolines to give *N*-aryl-1-amino indoles, *Org. Lett.*, **2021**, *23*, 6417–6422. [[Crossref](#)], [[Google Scholar](#)], [[Publisher](#)]
- [15] T. Yang, H. Lu, Y. Shu, Y. Ou, L. Hong, C.-T. Au, R. Qiu, CF₃SO₂Na-mediated, UV-light-induced Friedel–Crafts alkylation of indoles with ketones/aldehydes and bioactivities of products, *Org. Lett.*, **2020**, *22*, 827–831. [[Crossref](#)], [[Google Scholar](#)], [[Publisher](#)]
- [16] L.C. Chou, L.J. Huang, J.S. Yang, F.Y. Lee, C.M. Teng, S.C. Kuo, Synthesis of furopyrazole analogs of 1-benzyl-3-(5-hydroxymethyl-2-furyl) indazole (YC-1) as novel anti-leukemia agents, *Bioorg. Med. Chem.*, **2007**, *15*, 1732–1740. [[Crossref](#)], [[Google Scholar](#)], [[Publisher](#)]
- [17] M.A. Abdulla, A.K. Salman, Synthesis and Anti-Bacterial Activities of a Bis-Chalcone Derived from Thiophene and Its Bis-Cyclized Products, *Molecules*, **2011**, *16*, 523-531. [[Crossref](#)], [[Google Scholar](#)], [[Publisher](#)]

- [18] E. Nassar, Synthesis, (in vitro) antitumor and antimicrobial activity of some pyrazoline, pyridine, and pyrimidine derivatives linked to indole moiety, *Am. J. Sci.*, **2010**, *6*, 338-347. [[Google Scholar](#)], [[Publisher](#)]
- [19] S.A. Rahman, Y. Rangjendra, K. Bhvvaneswari, P. Kumar, Synthesis and antihistaminic activity of novel pyrazoline derivatives, *Int. J. of Chem. Tech. Res.*, **2010**, *2*, 16-20. [[Google Scholar](#)], [[Publisher](#)]
- [20] M. Bauser, G. Delapierre, M. Hauswald, T. Flessner, D. D'Urso, A. Hermann, B. Beyreuther, J. De Vry, P. Spreyer, E. Reissmüller, Discovery and optimization of 2-aryl oxazolo-pyrimidines as adenosine kinase inhibitors using liquid phase parallel synthesis, *Bioorg. Med. Chem. Lett.*, **2004**, *14*, 1997-2000. [[Crossref](#)], [[Google Scholar](#)], [[Publisher](#)]
- [21] A. Sochacka-Cwikła, A. Regiec, M. Zimecki, J. Artym, E. Zaczynska, M. Kocięba, I. Kochanowska, I. Bryndal, A. Pyra, M. Mączyński, Synthesis and biological activity of new 7-amino-oxazolo[5,4-d]pyrimidine derivatives, *Molecules*, **2020**, *25*, 3558. [[Crossref](#)], [[Google Scholar](#)], [[Publisher](#)]
- [22] Y. Velihina, T. Scattolin, D. Bondar, S. Pilo, N. Obernikhina, O. Kachkovskiy, I. Semenyuta, I. Caligiuri, F. Rizzolio, V. Brovarets, Synthesis, in silico and in vitro evaluation of novel oxazolopyrimidines as promising anticancer agents, *Helv. Chim. Acta*, **2020**, *103*, e2000169. [[Crossref](#)], [[Google Scholar](#)], [[Publisher](#)]
- [23] Y.H. Deng, D. Xu, Y.X. Su, Y.J. Cheng, Y.-L. Yang, X.Y. Wang, J. Zhang, Q.D. You, L.P. Sun, Synthesis and biological evaluation of novel oxazolo[5,4-d]pyrimidines as potent VEGFR-2 inhibitors, *Chem. Biodivers.*, **2015**, *12*, 528-537. [[Crossref](#)], [[Google Scholar](#)], [[Publisher](#)]
- [24] M. Mączyński, A. Regiec, A. Sochacka-Cwikła, I. Kochanowska, M. Kocięba, E. Zaczynska, J. Artym, W. Kałas, M. Zimecki, Synthesis, physicochemical characteristics and plausible mechanism of action of an immunosuppressive isoxazolo[5,4-e]-1,2,4-triazepine derivative (RM33), *Pharmaceuticals*, **2021**, *14*, 468. [[Crossref](#)], [[Google Scholar](#)], [[Publisher](#)]
- [25] B. Łachor, U.; Ryng, S.; M. M. Mączyński, J. Artym, M. Kocięba, E. Zaczynska, I. Kochanowska, E. Tykarska, M. Zimecki, Synthesis, immunosuppressive properties, mechanism of action and X-ray analysis of a new class of isoxazole derivatives, *Acta Pol. Pharm. Drug. Res.*, **2019**, *76*, 251-263. [[Crossref](#)], [[Google Scholar](#)], [[Publisher](#)]
- [26] A. Płoszaj, A. Regiec, S. Ryng, A. Piwowar, M. Kruzel, Influence of 5-amino-3-methyl-4-isoxazolecarbohydrazide on selective gene expression in Caco-2 cultured cells, *Immunopharmacol. Immunotoxicol.*, **2016**, *38*, 486-494. [[Crossref](#)], [[Google Scholar](#)], [[Publisher](#)]
- [27] A. Drynda, B. Obminska-Mrukowicz, M. Mączyński, M.S. Ryng, The effect of 5-amino-3-methyl-4-isoxazolecarboxylic acid hydrazide on lymphocyte subsets and humoral immune response in SRBC-immunized mice, *Immunopharmacol. Immunotoxicol.*, **2015**, *37*, 148-157. [[Crossref](#)], [[Google Scholar](#)], [[Publisher](#)]
- [28] A.R. Katritzky, M. Yoshioka-Tarver, B.E. D.M. El-Gendy, C.D. Hall, Synthesis and photochemistry of pH-sensitive GFP chromophore analogs, *Tetrahedron Lett.*, **2011**, *52*, 2224-2227. [[Crossref](#)], [[Google Scholar](#)], [[Publisher](#)]
- [29] Z.S.M. Al-Garawi, I.H.R. Tomi, A.H.R. Al-Daraji, Synthesis and characterization of new amino acid-schiff bases and studies their effects on the activity of ACP, PAP and NPA enzymes (*In Vitro*), *J. Chem.*, **2012**, *9*, 962-969. [[Crossref](#)], [[Google Scholar](#)], [[Publisher](#)]
- [30] Y.F. Mustafa, Synthesis, characterization, and biomedical assessment of novel bisimidazole-coumarin conjugates, *Appl. Nanosci.*, **2021**. [[Crossref](#)], [[Google Scholar](#)], [[Publisher](#)]
- [31] T.S. Kadhim, M.M. Kareem, A.J. Atiyah, Synthesis, characterization and investigation of antibacterial activity for some new functionalized luminol derivatives, *Bull. Chem.*

Soc. Ethiop., **2023**, *37*, 159-169. [[Crossref](#)], [[Google Scholar](#)], [[Publisher](#)]
[32] I.A. Mohammed, M.M. Kareem, Synthesis, characterization and study of some of new mefenamic acid derivatives as cytotoxic agents, *Journal of Physics: Conference Series*, **2020**, *1664*, 012081. [[Crossref](#)], [[Google Scholar](#)], [[Publisher](#)]

How to cite this article: Hayfaa A.Mubarak, Alaa Ali Hussein, Wisam Abdul Jaleel Jawad, Mustafa M.Karhib, Nour Abd Alrazzak, Mohanad Mousa Kareem. Synthesis of new indole derivatives as antibacterial and antitumor candidates. *Eurasian Chemical Communications*, 2023, *5*(5), 411-424. **Link:** http://www.echemcom.com/article_165822.html